Published September 1, 1983

Scanning Electron Microscope-Analysis of the Protrusions (Knobs) Present on the Surface of *Plasmodium falciparum*-infected Erythrocytes

JEAN GRUENBERG, DAVID R. ALLRED, and IRWIN W. SHERMAN
Department of Biology, University of California, Riverside, California 92521. Dr. Gruenberg's present address is European Molecular Biology Lab, 6900 Heidelberg, Federal Republic of Germany.

ABSTRACT The nature of the surface deformations of erythrocytes infected with the human malaria parasite *Plasmodium falciparum* was analyzed using scanning electron microscopy at two stages of the 48-h parasite maturation cycle. Infected cells bearing trophozoite-stage parasites (24–36 h) had small protrusions (knobs), with diameters varying from 160 to 110 nm, and a density ranging from 10 to 35 knobs $\times \mu m^{-2}$. When parasites were fully mature (schizont stage, 40–44 h), knob size decreased (100-70 nm), whereas density increased (45–70 knobs $\times \mu m^{-2}$). Size and density of the knobs varied inversely, suggesting that knob production (*a*) occurred throughout intraerythrocytic parasite development from trophozoite to schizont and (*b*) was related to dynamic changes of the erythrocyte membrane. Variation in the distribution of the knobs over the red cell surface was observed during parasite maturation. At the early trophozoite stage of parasite development, knobs appeared to be formed in particular domains of the cell surface. As the density of knobs increased and they covered the entire cell surface, their lateral distribution was dispersive (more-than-random); this was particularly evident at the schizont stage. Regional surface patterns of knobs (rows, circles) were seen throughout parasite development. The nature of the dynamic changes that occurred at the red cell surface during knob formation, as well as the nonrandom distribution of knobs, suggested that the red cell cytoskeleton may have played a key role in knob formation and patterning.

The surface of the erythrocyte infected with mature asexual stages (trophozoites and schizonts) of *Plasmodium falciparum* is altered by small excrescences called knobs (1–4). By transmission electron microscopy, knobs appear as electron-dense masses lying beneath a local protrusion of the red cell plasma membrane; in some instances the unit structure of the red cell plasma membrane is obscured (4). Knobs are believed to be involved in the occlusive vascular pathology of malaria (4–6) since schizont-infected erythrocytes are sequestered in the deep tissue capillaries of the host, and recent in vitro studies have shown an increased binding affinity of knobby erythrocytes to endothelial cells (7).

The manner whereby knob formation in *P. falciparum*-infected red cells occurs remains unknown. Some workers contend that parasite proteins are inserted into the host cell membrane and that this results in surface deformations. Indeed, parasite proteins have been detected in the membranes of red cells infected with the monkey parasite *P. knowlesi* (8–11). In *P. falciparum*-infected cells an 80,000-dalton parasite protein was reported to be the knob protein, since this protein was present in parasite cultures that induced knob formation and was absent from cultures that did not induce knobs (12). In addition, since knobs bind ferritin-labeled antibodies either derived from the sera of immune monkey (13) or raised against "purified" parasites (14) it has been suggested that knobs bear plasmodial antigens. Despite their obvious appearance, as well as the physiologic/pathologic significance of knobs, a detailed study of knob distribution on the surface of the *P. falciparum*-infected cell has not been carried out. The aim of the present study was to characterize, by scanning electron microscopy, how knob size and density vary as a function of parasite development and to determine whether there were characteristic patterns in the distribution of these excrescences. A statistical analysis was carried out to determine whether the lateral distribution of knobs was random, or in some way ordered.

Published September 1, 1983

MATERIALS AND METHODS

Parasite and Cultivation: Two clones of *P. falciparum* (FCR-3 Gambia strain) were used in this study. One produces knobs on the surface of the infected red cell and the other does not. Both were kindly provided by Dr. L. H. Miller (National Institutes of Health, Bethesda, MD).

Parasites were grown in vitro according to the methods of Trager and Jensen (15). The medium consisted of RPMI-1640 tissue culture medium supplemented with 0.2% (wt/vol) sodium bicarbonate, 25 mM HEPES, and 10% (vol/vol) normal human serum. Parasite development was synchronized according to the technique of Lambros and Vanderberg (16).

Isolation of Schizont-infected Erythrocytes: Synchronized cultures of *P. falciparum*-infected erythrocytes at a parasitemia of 5%, with 50% of the parasites at the multinucleate schizont stage were collected by centrifugation (1,500 *g*, 7 min) and then separated on a Percoll-Hypaque gradient modified from Vettore et al. (17). Typically, a 0.4-ml pellet of packed red cells was resuspended in the gradient mixture (3.5 ml of Percoll, 1.6 ml of Hypaque 75, 1.0 ml of 0.1 M sodium phosphate buffer pH 7.1, 3.5 ml of H_2O) and centrifuged (35,000 *g*, 20 min) in a Sorvall SS-34 rotor (DuPont Instruments, Sorvall Biomedical Div., DuPont Co., Wilmington, DE). The uppermost fraction of the gradient (Fig. 1) was recovered, diluted 1:10 with PBS (10 mM sodium-phosphate, 0.85% (wt/vol) NaCl, pH 7.4), and centrifuged (1,500 *g*, 10 min). The pellet (~50 μl of packed cells) containing schizont-infected erythrocytes was washed two times in PBS (1,500 *g*, 7 min) and immediately processed for prefixation (see below).

Isolation of Trophozoite-infected Erythrocytes: Red cells infected with synchronized trophozoites and with a parasitemia varying from 8 to 10% were collected by centrifugation (1,500 *g*, 7 min). The infected red cells were then concentrated using physiogel according to a procedure modified from Pasvol et al. (18). Briefly, a 25% suspension of red cells in complete culture medium was mixed with an equal volume of physiogel. After 30 min at 37°C, the supernatant, enriched in trophozoite-stage parasites, was recovered and centrifuged (1,500 *g*, 7 min). The red cell pellet was washed two times in PBS (1,500 *g*, 7 min) and then processed as described below.

Prefixation: Infected red cells bearing either trophozoites or schizonts (recovered by physiogel sedimentation or Percoll-Hypaque gradient centrifugation, respectively) were prefixed for 10 min at room temperature with 0.1% (vol/vol) glutaraldehyde in PBS according to Turner and Liener (19). Then, the prefixed cells were washed five times in a low ionic strength buffer (250 mosM sucrose, 50 mosM sodium-phosphate, pH 7.1) and subsequently coupled to polycationic beads.

Coupling to Polycationic Beads: Polyacrylamide beads coated with polyethyleneimine (Affi-gel 731, Bio-Rad Laboratories, Richmond, CA) were used as a polycationic solid support. Beads were hydrated for 15 min in water, washed two times with 2 M NH_4Cl, two times with H_2O, and finally two times with the low ionic strength buffer. A 50% suspension of beads in low ionic strength buffer was added dropwise to an identical volume of a 50% cell suspension in the same buffer, as described by Jacobson (20) and Jacobson and Branton (21). The beads were then allowed to settle by gravity, and the supernatant containing the unbound cells was removed. Washing by gravity sedimentation in low ionic strength buffer was repeated twice.

Scanning Electron Microscopy: The beads, spread as a monolayer in a flat-bottomed glass dish, were fixed for 4 h at 4°C in 0.1 M sodium phosphate buffer, pH 7.4 containing 2% glutaraldehyde, 4% sucrose, and 2.10^{-5} M $CaCl_2$. The fixative was removed, and the beads were washed four times with 0.1 M sodium phosphate buffer, pH 7.4. After washing, the beads were dehydrated in a graded series of acetone, critical point dried using CO_2 as a transition fluid, mounted on aluminum stubs with silver paint, and coated with gold. Samples were examined in a JEOL JSM-35C scanning electron microscope.

Electron Micrograph Analysis: In both preparations (schizont- and trophozoite-infected erythrocytes) a large number of cells were randomly photographed at the same magnification (× 18,000). Knob size, density, and lateral distribution were measured on each cell using enlarged prints of the electron micrographs (final magnification 1 μm = 5.2 cm). Knob diameter was averaged by directly measuring 50–100 knobs/cell. Knob density and lateral distribution were obtained by placing a transparency over the micrograph so that knobs could be marked by a point on the transparency. Only flat areas of the red cell surface, i.e., those parallel to the plane of the micrograph and with only minor deformations and irregularities, were analyzed. To the transparency bearing the points, another transparency was then applied on which a grid had previously been created (mesh size, either 0.9 × 0.9 cm corresponding to an area of 0.03 μm^2 or 1.8 × 1.8 cm, corresponding to 0.12 μm^2). The number of knobs per square (either 0.03 μm^2 or 0.12 μm^2) was then determined for 50–500 squares/cell. From these data the average knob density per cell was calculated (total number of knobs/total number of squares) along with the frequency distribution of knob density (i.e., squares with no knobs, one knob, two knobs, and so on).

Deviation of knob lateral distribution from random was investigated by calculating the normal deviate (z-value) for each cell according to de Laat et al. (22). This analysis determines the probability that the observed frequency distribution differs from a Poisson distribution. Thus, absolute z-values of 1.65, 2.33, and 3.1 correspond to significance probabilities of 5, 1, and 0.1% respectively. A random distribution can be expected if $z = 0$; whereas $z > 0$ indicates aggregation, and $z < 0$, a more uniform than random distribution (dispersion).

Materials: Percoll was obtained from Pharmacia Fine Chemicals (Div. of Pharmacia, Inc., Piscataway, NJ) and Hypaque 75 was obtained from Winthrop Laboratories (New York, NY). RPMI-1640 was purchased from Gibco Laboratories (Grand Island, NY). HEPES was purchased from Calbiochem-Behring Corp., (La Jolla, CA). Physiogel was purchased from Hausman Laboratories (St. Gallen, Switzerland).

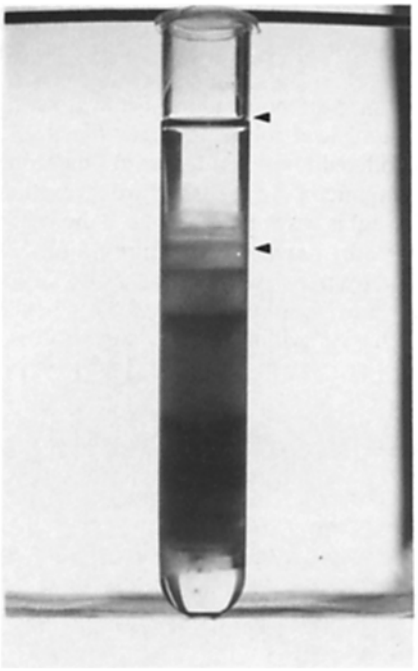

FIGURE 1 Percoll-Hypaque gradient. Schizont - infected erythrocytes were recovered as described in Materials and Methods from the uppermost fraction (between arrows).

RESULTS

Isolation of Infected Cells

Analysis of knob distribution on the surface of human erythrocytes infected with *P. falciparum* at the trophozoite and the schizont stages of asexual development required not only high parasitemias but a sharply defined range of parasite development. These two conditions were met by isolating synchronously growing schizont-infected erythrocytes on a Percoll-Hypaque density gradient as described in Materials and Methods (Fig. 1). This separation procedure, which depends on a change in cell density during parasite development, provided for excellent isolation of late schizont-infected cells from late trophozoite- and early schizont-infected cells (Fig. 1), as well as from the majority of uninfected cells (Fig. 2*a*). Routinely, a 70% parasitemia, with 80% of the parasites at the late schizont stage, could be recovered from the uppermost fraction of the gradient (Fig. 1). However, when trophozoite-infected cells were studied, these were isolated using physiogel sedimentation. Physiogel sedimentation for separation of trophozoite-infected erythrocytes depends on the presence of knobs on the cell surface. This being so, trophozoite-infected cells cannot be separated from later stages since both stages have knobs; therefore, synchronously growing cultures were applied to the physiogel before schizogony could be detected.

Published September 1, 1983

Using this scheme a population of red cells with 70% parasitemia, 90% of which were at the trophozoite stage, was recovered (Fig. 2*b*).

In both cases, the isolated subpopulation of infected cells was electrostatically bound to a solid support (Affi-gel 731 beads). This procedure offered two advantages: (*a*) Processing of the sample for electron microscopy (washings, dehydration series, critical point drying) is easy and quick since the beads are large enough to settle by gravity and require no further mounting of the sample (except for the stub itself); and (*b*) when examined under the microscope, the cells are well separated from each other, providing various angles of orientation.

It must be emphasized that the isolated infected erythrocytes were prefixed in 0.1% glutaraldehyde before coupling to the beads to prevent any cell surface damage from occurring during attachment. Indeed, uninfected cells appeared normal (Fig. 3) when coupled to the beads.

Changes in Knob Size and Density

Knobs were evident as small excrescences on the surface of the infected red cell (Fig. 4). The major deformations of the erythrocyte surface and shape will be discussed below. The

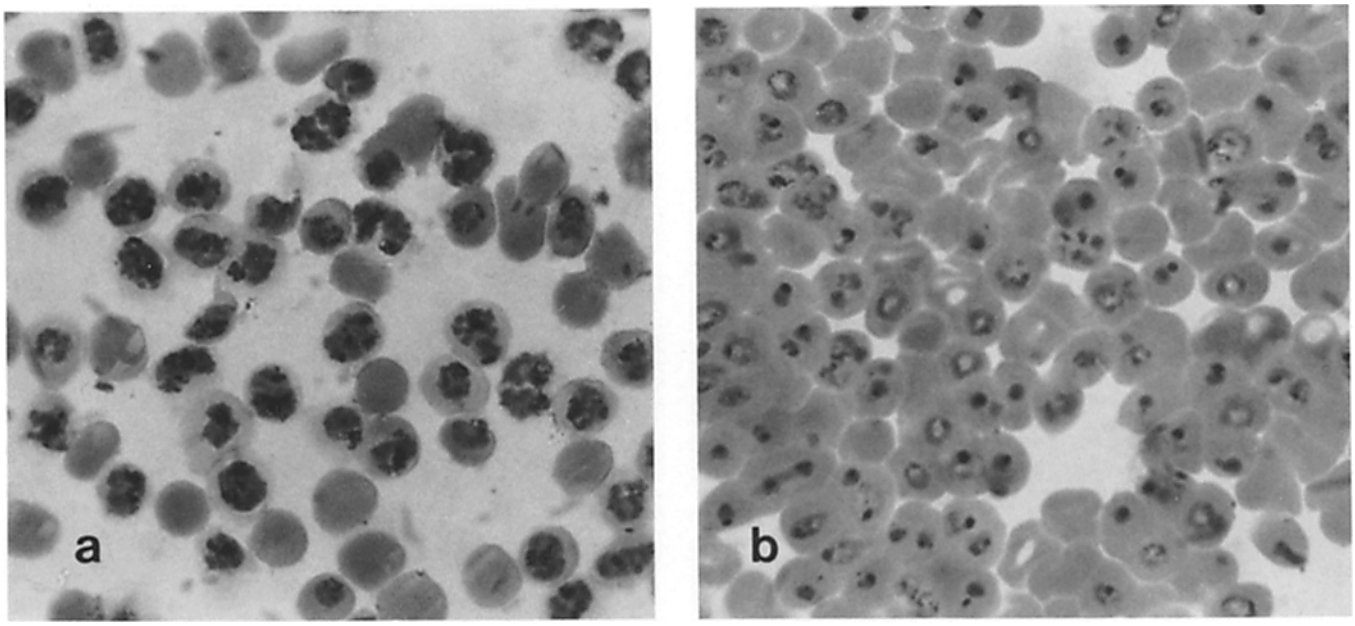

FIGURE 2 Giemsas'-stained smears. Purified schizont- (*a*) and trophozoite-infected (*b*) erythrocyte fractions collected, respectively, from the Percoll-Hypaque gradient and from the physiogel sedimentation procedure. (*a*) Total parasitemia was 70%, of which 80% were schizonts, 8% binucleates, 2% trophozoites, and 10% rings. (*b*) Total parasitemia was 73%, of which 5% were schizonts, 5% binucleates, and 90% trophozoites.

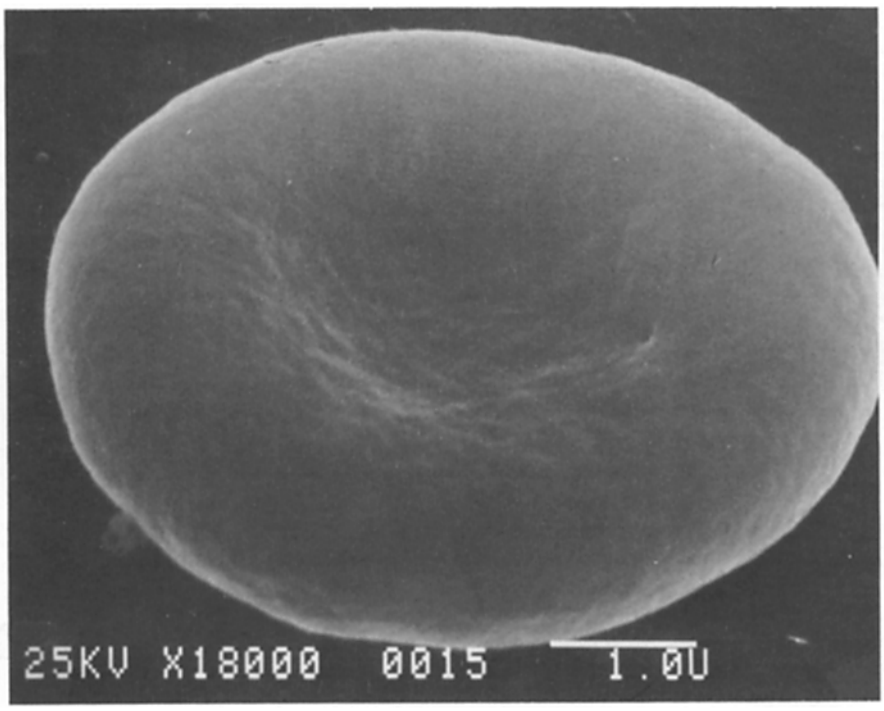

FIGURE 3 Uninfected erythrocyte. Scanning electron micrograph of an uninfected red cell (processed for electron microscopy identical to Fig. 4).

Published September 1, 1983

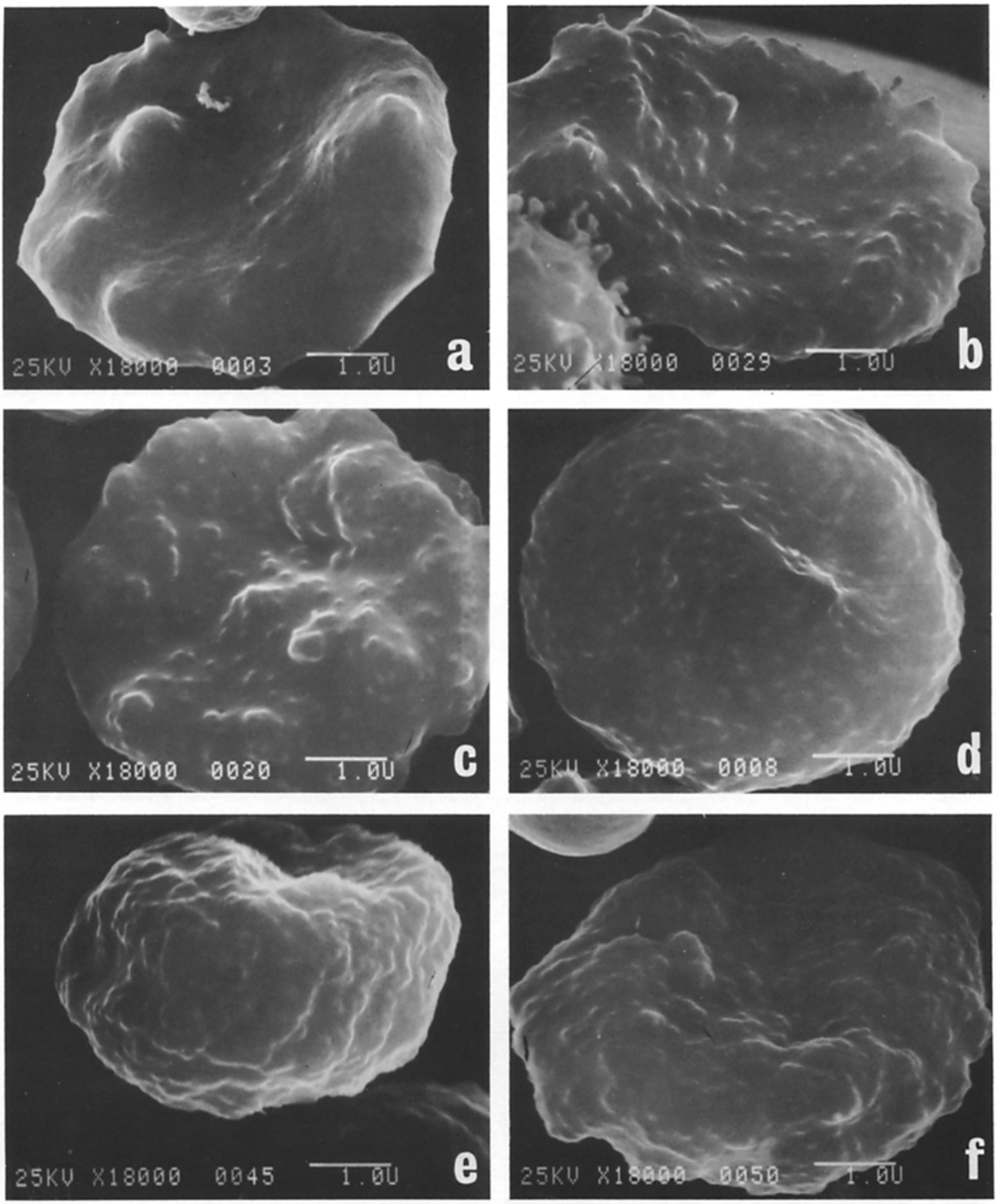

FIGURE 4 Trophozoite-infected and schizont-infected erythrocytes. The micrographs of the infected erythrocytes are ordered according to the increasing density of knobs on the cell surface (knobs × μm^{-2}). Namely, *a* (8), *b* (12), *c* (17), *d* (19), *e* (25), and *f* (30); *g* (39), *h* (48), *i* (56), *j* (62), *k* (64), and *l* (92). All micrographs are at the same magnification indicated by a bar of 1.0 μm in each micrograph.

average knob density and size changed dramatically during parasite maturation (Fig. 4). When knob size was plotted as a function of the average density (Fig. 5), an inverse relationship was evident: Knob size decreased as knob density increased. Unexpectedly, the populations of infected cells bearing the two developmental stages were well separated. At the tropho-

Published September 1, 1983

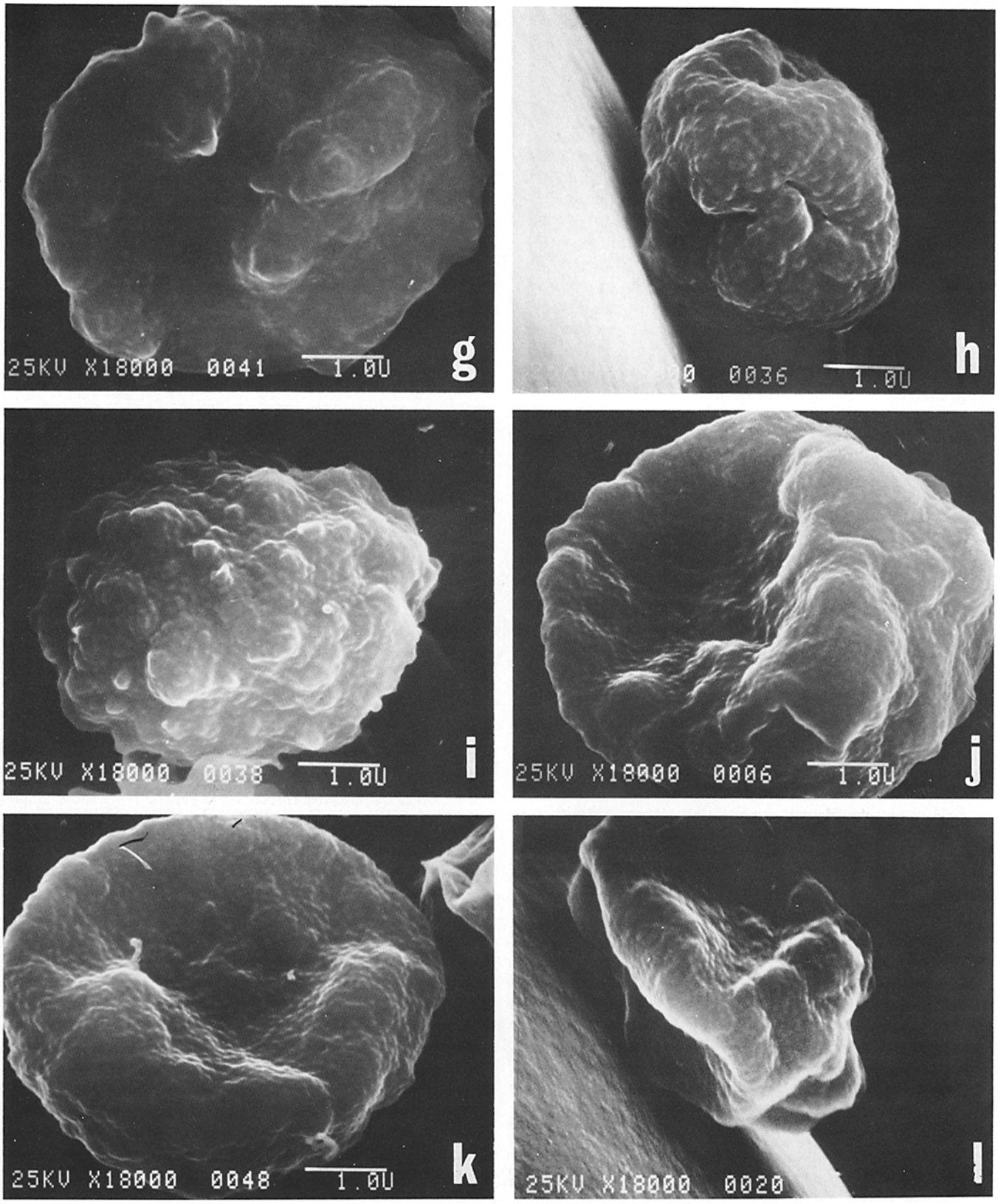

FIG. 4 *Continued.*

zoite stage, density varied from 10 to 35 knobs × μm^{-2} and knob diameter varied from 150 to 110 nm, whereas at the schizont stage the knob density ranged from 45 to 75 knobs × μm^{-2} and the size varied from 100 to 70 nm (only a few cells exhibited higher densities). It should be noted that in the trophozoite-infected cell preparations a few infected cells with knob densities and sizes characteristic of the schizont stage were present (and vice versa); this finding by scanning electron microscopy was consistent with light microscopic evidence from Giemsas'-stained smears (Fig. 2, *a* and *b*). Thus, despite

Published September 1, 1983

synchronization and the sedimentation-centrifugation procedures used, cross contamination with other stages could not be totally eliminated.

Lateral Distribution of Knobs

Overall knob distribution on the surface of cells infected with parasites at both stages of development was analyzed to determine whether there was a deviation from random. The frequency distributions of knob densities were calculated for all cells represented in Fig. 5 using a 0.12- and a 0.03-μm^2 mesh size at the trophozoite and schizont stages, respectively. Since knob size varied throughout parasite development, the particular mesh size used corresponded to a square with dimensions approximately three times the average diameter of the knobs at each stage, as suggested for this type of analysis (22). As an example, the frequency distributions obtained with the 0.03-μm^2 mesh size are shown in Fig. 6. The probability that the frequency distribution for each cell deviates from a Poisson distribution could be obtained from the z-value (5% significance for $|z| > 1.65$), showing either aggregation ($z > 0$) or dispersion ($z < 0$). In most cases, but especially at the schizont stage, a highly significant dispersive effect was observed: Knobs tended to be distributed over the erythrocyte surface as if they repelled each other (Table I). (The exceptional case of the trophozoite-infected cell showing the lowest knob density [(Fig. 4*a*)] will be discussed in the next section.)

Patterns of Knob Distribution

A closer examination of the infected red cell surface, especially with parasites at the trophozoite stage, revealed distinct patterns of knob distribution. The following patterns, though not exhibited over the entire cell surface, were evident on all cells. (*a*) Knob domains. Cells bearing fewer knobs (Fig. 4, *a–c*) showed an increased density of knobs in particular domains of the cell surface. Infected erythrocytes generally exhibited local deformations of their surface (bumps; see Discussion)

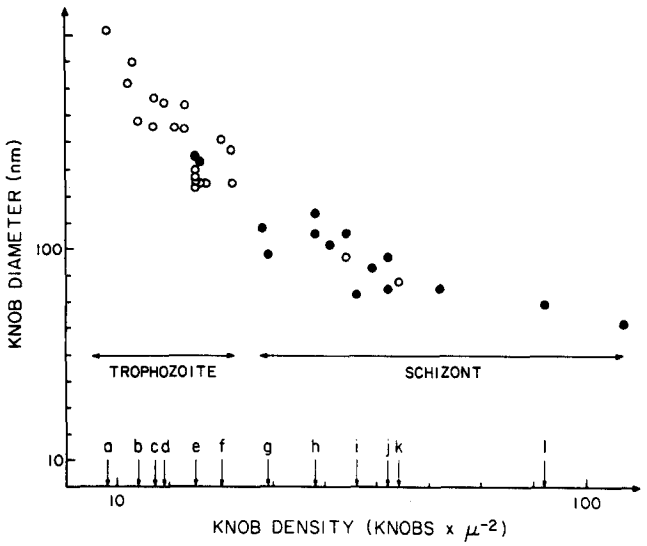

FIGURE 5 Variation of knob size and density. Knob diameter (*y*-axis) and density (*x*-axis) were determined for each erythrocyte in the preparation of trophozoite- (open symbols) and schizont-infected erythrocytes (closed symbols), as described in Materials and Methods. Arrows on the *x*-axis point to the density corresponding to the cells shown in Fig. 4.

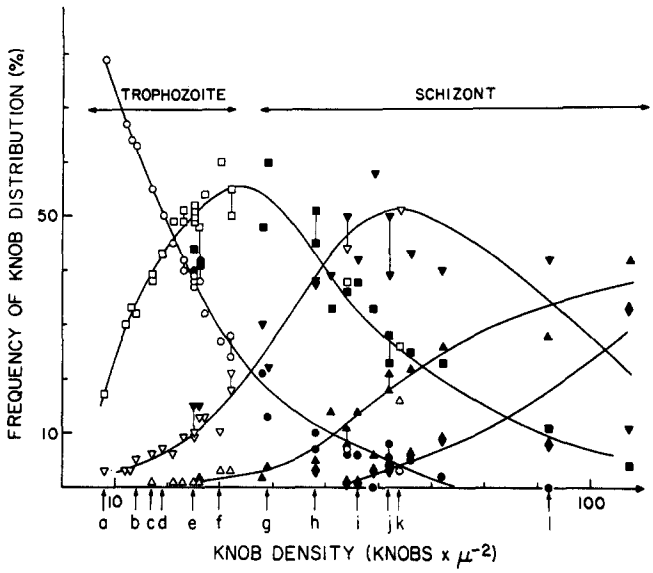

FIGURE 6 Knobs frequency distribution. For each cell the knob frequencies were expressed as the percent of the total number of 0.03 μm^2 squares bearing no knobs (circles), 1 knob (squares), 2 knobs (triangles pointing downward), 3 knobs (triangles pointing upward), and 4 knobs (diamonds), as described in Materials and Methods. The frequencies (*y*-axis) are shown as a function of knob density (*x*-axis). Symbols and arrows on the *x*-axis as in Fig. 5. Each frequency class (no knobs, 1 knob, and so on) in 0.03-μm^2 squares reaches a maximum at a given range of knob density, and, when knob density increases, knob distribution is shifted towards higher frequency classes.

when compared to normal cells (Fig. 3); these deformations were more extensive at later stages of parasite development (Fig. 4, *g–l*). Knobs also appeared to be present at a higher density on bumps (Fig. 4*c*). In Fig. 4*a*, due to the very low knob density, the knob domains were even more obvious and accounted for the highly significant positive z-value (Table I). In the other trophozoite-infected cells (Fig. 4, *b–f*), the average density of the knobs was higher and they were more evenly distributed over the cell surface, showing an overall tendency towards dispersion (Table I). (*b*) Clusters. Close association of two or more knobs, arranged in clusters, was often observed particularly on bumps (Fig. 4). This clustering of knobs was observed even with younger stages (including Fig. 4*a*) when the average knob density was low. Knobs were so closely associated within a cluster that sometimes the individual knobs were impossible to distinguish from one another. (*c*) Linear and circular patterns. Particularly with the earlier stages of parasite development (Fig. 4, *a–f*), but also at later stages (Fig. 4, *g–l*), knobs appeared to be arranged in parallel rows (Fig. 4*h*, center) or converged to form a Y-shape (Fig. 4*b*, center). Knobs also appeared to be arranged in circles of seven to ten knobs throughout parasite development, especially in regions where there were bumps on the cell surface (Fig. 4, *e* and *k*); however, this was not always the case (Fig. 4, *j*, center of depression).

DISCUSSION

Major Cell Deformations

Erythrocytes infected with late asexual developmental stages of *P. falciparum* showed drastic alterations in their morphology (Fig. 4) in addition to knob formation, when compared to uninfected cells (Fig. 3). These major surface

Published September 1, 1983

TABLE I
Knob Distribution

Developmental stage	Cells (Fig. 4)	Density (knobs × μm^{-2})	z-Value 0.03 μm^{2*}	z-Value 0.12 μm^{2*}
Trophozoite-infected erythrocytes	a	8		+6.9
		12		−1.7
		13		−2.4
	b	14		−2.0
		17		−1.0
	c	17		−1.2
	d	19		−3.2
		21		−1.8
		23		−2.0
		23		−2.1
		25		−2.1
‡		25		−1.0
		25		−2.5
	e	25		−2.7
		25		−3.1
‡		26		ND
		26		−1.1
		27		−3.8
	f	30		−2.2
		32		−3.5
		32		−1.5
Schizont-infected erythrocytes		38	−3.2	
	g	39	−4.6	
	h	48	−4.3	
		48	−3.9	
		51	−2.2	
		54	−3.5	
§		54	−6.9	
	i	56	−4.2	
		59	−4.0	
		62	−3.7	
	j	62	−5.2	
§	k	64	−7.5	
		66	−4.8	
		72	−3.8	
	l	92	−1.6	
		107	−4.3	

ND: Not determined.
* Mesh size.
‡ Infected cells isolated in experiments carried out at the schizont stage.
§ Infected cells isolated in experiments carried out at the trophozoite stage.

deformations did not appear to be a direct consequence of knob production since they were also observed on erythrocytes infected with a clone derived from the same strain of *P. falciparum,* but which did not induce knob formation (data not shown). However, it remains unresolved whether these deformations were the result of parasitization or whether they were an artifactual consequence of processing for electron microscopy, or from metabolic stress due to long-term culture in vitro. Although malaria-infected red cells are known to be "leaky" (23, 24) and osmotically fragile (25, 26), especially schizont-infected cells, the possibility that these deformations may have been present in vivo should be considered in view of the fact that the infected cells were prefixed immediately after isolation. Trager et al. (27) reported that knobs could be seen on live material by video-enhanced differential interference contrast microscopy. However, the diameter of the alterations on the surface of infected cells was an order of magnitude larger than the recorded diameter of the knobs (this work and transmission electron microscopy, 1–4), making it highly likely that these protuberances (see Fig. 4) were bumps, not knobs.

Whether these bumps occur naturally or are artifactual is of little consequence to the present study of knob distribution since only those surface areas devoid of such alterations were analyzed, and our primary concern was with the general aspects of knob size and density variation rather than a detailed morphological description of each case.

Knob Density and Size

As seen in Fig. 5, trophozoite-infected erythrocytes exhibited fewer large knobs than did schizont-infected cells; this was in contrast to the results of Langreth et al. (4), which were based on a limited number of thin sections observed by transmission electron microscopy. From the data presented in Fig. 5, it is tempting to correlate the variations in knob density and size with the stage of intraerythrocytic parasite development. Although it is possible to assign a particular stage in the developmental cycle to a group of cells that exhibited similar densities and sizes (Fig. 5), it is impossible to precisely determine the stage of parasite development for an individual cell since no information regarding the parasite itself can be obtained using the present procedures. It is also impossible to ascertain what (if any) the effects of multiple infection were on knob production in a single erythrocyte.

However, it did appear that knobs were not produced continuously or uniformly throughout parasite maturation. The population of trophozoite-infected cells used for this study represented a broader range of developmental stages than did the schizont-infected cells: Trophozoite maturation took 12 h of the 48-h asexual developmental cycle whereas schizont maturation occurred in 6 h, and the isolation procedures used allowed purification of late schizonts (Percoll-Hypaque gradient), whereas all stages of trophozoite-infected cells were isolated using physiogel sedimentation. Yet both populations, as shown in Fig. 5, had similar ranges of knob densities (~20–30 knobs × μm^{-2}), suggesting that at later stages of parasite development the rate of knob production increased.

Spatial Distribution of Knobs

Knobs appeared not to be randomly distributed over the surface of the infected red cell. Evidence for this came from both the particular patterns (rows, circles, knob domains) formed by the knobs (Fig. 4) and the general tendency of knobs to be or[illegible]ized in a more-than-random manner (dispersive) (Table I). Specific knob patterns were more obvious at the trophozoite stage when the average knob density was lower, implying that knobs might have first been produced in specific domains of the membrane (See Fig. 4, *a–c*). Then, when knob density increased, they tended to cover the entire erythrocyte surface, and showed a stronger dispersive tendency (Table I).

The statistical analysis used in the present study was based on a determination of the degree to which a given distribution of frequencies deviated from a Poisson distribution. Since such an analysis applied accurately only for a spatial distribution of points accounting for a negligible portion (5%) of the field analyzed (22), it was necessary to use areas of the cell surface that were flat and showed only minor deformations. Knobs appeared to cover >5% of the cell surface,

varying from 15 (Fig. 4*b*) to 25% (Fig. 4*k*) calculated from: $10^2 \times$ knob density $\times \pi \times$ (knob radius)^2/mesh size (0.03 μm^2 and 0.12 μm^2, respectively). However, transmission electron micrographs of knobs showed that the electron-dense material located beneath the plasma membrane, which presumably was responsible for the local deformation (protrusion), was approximately half the diameter of the total protrusion (1, 2, 4). This observation helps to explain the formation of knob clusters (Fig. 4) where knobs were found in close contact with one another. The distance separating two knobs in a cluster was up to ½ (or less) their average diameter. The electron-dense masses occupied an area beneath the membrane much smaller than the observed values (15–25%), and therefore were amenable to the statistical analysis used. This observation holds true for the determination of the overall organization of knob distribution as carried out in the present study; an analysis based on the comparison of the z-values from one cell to another was, however, beyond the limits of resolution of the system used.

In conclusion, knob formation on the infected cell surface appeared to be a dynamic process: Changes in size, density, and distribution occurred with parasite maturation. Such events implied a continuous reorganization-redistribution of membrane constituents, especially those cytoskeletal proteins responsible for red cell membrane stability. This dynamic process was likely to be the result of parasite-provoked damage inflicted on the infected cell membrane during parasite maturation. Although no direct evidence is yet available, there are many reports and observations consistent with such disruption of the cytoskeleton as a result of the malarial infection.

The fact that not all malarias induce knob formation and that the major alterations of the cell surface (bumps) are also seen on cells infected with a clone of *P. falciparum* that does not induce knobs indicates that several levels of modification are likely to be involved in knob formation, including some that remain completely unknown.

The helpful suggestions and comments of K. Yamada throughout the present study are greatly acknowledged.

This work was supported by a grant from the UNDP/World Bank/World Health Organization Special Program for Research and Training in Tropical Diseases, and a research grant from the National Science Foundation (PCM 78-22126).

Received for publication 29 November 1982, and in revised form 22 April 1983.

REFERENCES

1. Aikawa, M., and C. R. Sterling. 1974. Intracellular Parasitic Protozoa. Academic Press, Inc., New York. 1–76.
2. Trager, W., M. A. Rudzinska, and P. C. Bradbury. 1966. The fine structure of *Plasmodium falciparum* and its host erythrocyte in natural malarial infections in man. *Bull. W. H. O.* 35:883–885.
3. Luse, S. A., and L. H. Miller. 1971. *Plasmodium falciparum* malaria: ultrastructure of parasitized erythrocytes in cardiac vessels. *Am. J. Trop. Med Hyg.* 20:655–660.
4. Langreth, S. G., J. B. Jensen, R. T. Reese, and W. Trager. 1978. Fine structure of human malaria *in vitro*. *J. Protozool.* 25:443–452.
5. Miller, L. H. 1969. Distribution of mature trophozoites and schizonts of *Plasmodium falciparum* in the organs of *Aotus trivergatus*, the night monkey. *Am. J. Trop. Med. Hyg.* 18:860–865.
6. Miller, L. H., G. W. Cooper, S. Chien, and H. N. Freemount. 1972. Surface charge on *Plasmodium knowlesi*- and *Plasmodium coatneyi*- infected red cells of *Macaca mulatta*. *Exp. Parasitol.* 32:86–95.
7. Udeinya, I. J., J. A. Schmidt, M. Aikawa, L. H. Miller, and I. Green. 1981. *Falciparum* malaria-infected erythrocytes specifically bind to cultured human endothelial cells. *Science* (*Wash. DC*). 213:555–557.
8. Schmidt-Ullrich, R., D. F. H. Wallach, and J. Lightholder. 1980. Metabolic labeling of *Plasmodium knowlesi*-specific glycoproteins in membranes of parasitized rhesus monkey erythrocytes. *Cell Biology International Reports.* 4:555–561.
9. Wallach, D. F. H., and M. Conley. 1977. Altered membrane proteins of monkey erythrocytes infected with simian malaria. *J. Mol. Med.* 2:119–136.
10. Shakespeare, P. G., P. I. Trigg, and L. Tappenden. 1979. Some properties of membranes in the simian malaria parasite *Plasmodium knowlesi*. *Ann. Trop. Med. Parasitol.* 73:333–343.
11. Trigg, P. I., S. I. Hirst, P. G. Shakespeare, and L. Tappenden. 1977. Labelling of membrane glycoproteins in erythrocytes infected with *Plasmodium knowlesi*. *Bull. W. H. O.* 55:205–209.
12. Kilejian, A. 1979. Characterization of a protein correlated with the production of knob-like protrusions on membranes of erythrocytes infected with *Plasmodium falciparum*. *Proc. Natl. Acad. Sci. USA.* 76:4650–4653.
13. Langreth, S. G., and R. T. Reese. 1979. Antigenicity of the infected-erythrocyte and merozoite surfaces in *falciparum*-malaria. *J. Exp. Med.* 150:1241–1254.
14. Kilejian, A., A. Abati, and W. Trager. 1977. *Plasmodium falciparum* and *Plasmodium coatneyi*: immunogenicity of "knob-like protrusions" on infected erythrocyte membrane. *Exp. Parasitol.* 42:157–164.
15. Trager, W., and J. B. Jensen. 1976. Human malaria parasites in continuous culture. Science (*Wash. DC*). 193:673–675.
16. Lambros, C., and J. P. Vanderberg. 1980. Synchronization of *Plasmodium falciparum* erythrocytic stages in culture. *J. Parasitol.* 65:418–420.
17. Vettore, L., M. Concetta de Matteis, and P. Zampini. 1980. A new density gradient system for the separation of human red blood cells. *Am. J. Hematol.* 8:291–297.
18. Pasvol, G., R. J. M. Wilson, M. E. Smalley, and J. Brown. 1978. Separation of viable schizont-infected red cells of *Plasmodium falciparum* from human blood. *Ann. Trop. Med. Parasitol.* 72:87–88.
19. Turner, R. H., and I. E. Liener. 1975. The use of glutaraldehyde-treated erythrocytes for assaying the agglutinating activity of lectins. *Anal. Biochem.* 68:651–653.
20. Jacobson, B. S. 1980. Improved method for isolation of plasma membrane on cationic beads. Membranes from *Dictyostelium discoideum*. *Biochim. Biophys. Acta.* 600:769–780.
21. Jacobson, B. S., and D. Branton. 1976. Plasma membrane: rapid isolation and exposure of the cytoplasmic surface by use of positively charged beads. Science (*Wash. DC*). 195:302–304.
22. de Laat, S. W., L. G. J. Tertoolen, and J. G. Bluemink. 1981. Quantitative analysis of the numerical and lateral distribution of intramembrane particles in freeze-fractured biological membranes. *Eur. J. Cell Biol.* 23:273–279.
23. Kutner, S., D. Baruch, H. Ginsburg, and Z. I. Cabantchik. 1982. Alterations in membrane permeability of malaria-infected human erythrocytes are related to the growth stage of the parasite. *Biochim. Biophys. Acta.* 687:113–117.
24. Sherman, I. W. 1979. Biochemistry of *Plasmodium* (malarial parasites). *Microbiol. Rev.* 43:453–495.
25. Overman, R. R., A. C. Bass, and T. H. Tomlison, Jr. 1950. Ionic alterations in chickens infected with *Plasmodium gallinaceum*. *Fed. Proc.* 9:96–97.
26. Herman, R. 1969. Osmotic fragility of normal duck erythrocytes as influenced by extracts of *Plasmodium lophurae*, *P. lophurae*-infected cells and plasma. *J. Parasitol.* 55:626–632.
27. Trager, W., H. S. Stanley, R. D. Allen, and N. S. Allen. 1982. Knobs on the surface of erythrocytes infected with *Plasmodium falciparum*: visualization by video-enhanced differential interference contrast microscopy. *J. Parasitol.* 68:332–333.